

# Analysis of Chemical Composition of Gases from Rock Samples by Pulsed Discharge Chromatography Combined Mass Spectrometry

Liwu Li<sup>a,\*</sup>, Yan Liu<sup>a</sup>, Chunhui Cao<sup>a</sup>, Zhongping Li<sup>a</sup>, Lantian Xing<sup>a</sup>, Mingjie Zhang<sup>b</sup>, and Xianbin Wang<sup>a</sup>

<sup>a</sup>Key Laboratory of Petroleum Resources Research, Institute of Geology and Geophysics, Chinese Academy of Sciences, Lanzhou, 730000 China

<sup>b</sup>School of Earth Sciences, Lanzhou University, Lanzhou, 730000 China

\*e-mail: llwu@lzb.ac.cn

Received January 1, 2019; revised June 27, 2019; accepted August 8, 2019

**Abstract**—Understanding the chemical composition of gases trapped in rocks is important in a wide variety of earth science studies and gases are often extracted from rock samples and analyzed. Gas chromatography (GC) and mass spectrometry (MS) are the most frequently used analytical techniques for measuring gases extracted from rock samples, but these techniques have rarely been coupled except for gas chromatography-mass spectrometry (GC-MS) or Continuous flow isotope ratio mass spectrometry (CF-IRMS). A thermal conductivity detector (TCD) is most frequently used in GC because of its ability to detect all gases, but has limited sensitivity and thus cannot accurately detect trace gases in some rock samples. To resolve this issue, we built a new device that tests gases extracted from rock samples by GC and MS together, and employs a pulsed discharge detector (PDD) with GC analyses rather than a TCD because PDD is capable of detecting most gases and exhibits higher sensitivity than that of TCD. In this device, a rock sample can be heated or crushed in vacuum to release gases. A diaphragm gauge is then used to measure the pressure of the gases released from the rock samples. Four kinds of samples were tested using this new device: serpentinized peridotites from Inner Mongolia, volcanic rocks from Wudalianchi, shale rocks from Sichuan basin and reservoir rocks from Songliao basin. The chemical contents of H<sub>2</sub>, CH<sub>4</sub>, H<sub>2</sub>O, CO, N<sub>2</sub>, C<sub>2</sub>H<sub>4</sub>, C<sub>2</sub>H<sub>6</sub>, O<sub>2</sub>, H<sub>2</sub>S, Ar, CO<sub>2</sub>, C<sub>3</sub>H<sub>8</sub>, COS and SO<sub>2</sub> could be measured simultaneously.

**Keywords:** Trace gases in rocks, Step Crushing, Step heating, Degassing in high vacuum, Simultaneous measurement of GC and MS

**DOI:** 10.1134/S0016702920080078

## 1. INTRODUCTION

There are many volatile elements in Earth's interior, such as carbon, oxygen, hydrogen, nitrogen, and sulfur. During chemical interactions within Earth's interior, volatile elements rise to the surface of the Lithosphere, and either degas from the earth's interior or become preserved in rocks and minerals. The majority of degassing occurs via volcanism, during earthquakes, and emissions from hot springs, and much work has been done to study these phenomena (e.g., Fischer and Marty, 2005; Zheng et al., 2013; Menard et al., 2014; Queißer et al., 2017; Toki et al., 2017; Zhang et al., 2017). When volatile elements are preserved in rock, they form fluid inclusions or dissolve in rocks and minerals. Much work has been done to analyze fluid inclusions and volatile elements in rocks and minerals, with analytical techniques ranging from microscopic infrared spectroscopy, to laser Raman spectroscopy and ion probe spectroscopy, to micro thermometry (e.g., Frezzotti et al., 2012; Doucet et al., 2014; Armstrong et al., 2015; Clay et al., 2015; Mi et al., 2016). Studying volatile elements and

the compounds in which they are found has helped gain a better understanding of the composition of the primitive mantle, the circulation of the crust and mantle, the seismic activity of volcanoes, the origin of abiogenic natural gas and the origin of life (e.g., Colin and Marty, 2013; Klein et al., 2013; Pearson et al., 2014; Wang et al., 2014; Halldórsson et al., 2016). Analyzing the chemical composition of gas in source rock, oil reservoirs, gas reservoirs, and shale also provides important basic information in the study of oil and gas resources.

Two types of methods are used to analyze fluid inclusions and volatile elements in rocks and minerals: non-destructive methods and destructive methods. Non-destructive methods, such as Raman spectroscopy, Fourier transform infrared spectroscopy, and secondary ion mass spectrometry, can only detect the main gas components in the rock under the current condition (Pearson et al., 2014; Esposito et al., 2014). Thermometry, another non-destructive method, requires calculations to determine the main gas components of fluid inclusions.

For the study of trace gases in rocks, destructive methods that involve rock degassing are required. Heating and crushing are two destructive methods frequently used for extracting gases from rock or mineral samples (Marty and Humbert, 1997; Salvi and Williams-Jones, 2003; Dublyansky, 2012; Buikin et al., 2016). Gas chromatographs and mass spectrometers are the two instruments most frequently used for analysis of fluid inclusion volatiles (Salvi and Williams-Jones, 2003; Dublyansky, 2012). The gases released from rocks or minerals include but are not limited to  $H_2$ , He,  $CH_4$ ,  $H_2O$ , Ne, CO,  $N_2$ ,  $C_2H_4$ ,  $C_2H_6$ ,  $O_2$ ,  $H_2S$ , Ar,  $CO_2$ ,  $C_3H_8$ , and  $SO_2$  (Liu et al., 1997; Zhang et al., 2007; Tang et al., 2013). Liu et al. (1997) studied the chemical composition of gas from mantle xenoliths in alkali-basalt from Damaping, Hebei, China by step heating mass spectrometry. Salvi and Williams-Jones (2003) summarized the extraction and instrument testing of gas in fluid inclusions, noting that the main methods of gas extraction from fluid inclusions are heating and crushing. The measurement methods for determining the chemical composition of gas are mass spectrometry (MS) and gas chromatography (GC), GC-MS is also frequently used (Mulder et al., 2013; Sokol et al., 2017). CF-IRMS has been used to analyze the carbon/hydrogen isotopic compositions of volatile components of fluid inclusions (Potter and Longstaffe, 2007). Each of these techniques has advantages and disadvantages (Mironova, 2010).

Usually, either GC or MS is used to analyze gas compositions alone, and they are rarely combined, except in GC-MS or CF-IRMS. For these two combined methods, the gas chromatograph acts as a gas separation device and the mass spectrometer is used as the detector.

GC and MS have their own advantages and disadvantages. Despite its usefulness for particular applications, GC has several shortcomings. First, some compounds cannot be detected by chromatography. Second, the most common detectors have sensitivity and detection trade-offs: thermal conductivity detectors (TCD) have low sensitivity but can detect all gasses, while selective detectors like flame ionization detectors (FID) are more sensitive but only respond to specific compounds. Third, some compounds such as Ar and  $O_2$  are difficult to separate by column chromatography. MS is sensitive to almost all compounds, but cannot effectively separate the same or similar molecular weight ions (e.g.  $CO^+$ ,  $N_2^+$  and  $C_2H_4^+$ ). One may use mathematical methods to deal with MS spectra (Blamey et al., 2012), but these methods are challenging when there are only a few MS peaks.

To accommodate the aforementioned limitations of each instrument, we built a new device. In this device, gases are extracted from rock samples and tested by GC and MS together. Instead of TCD or FID, a pulsed discharge detector (PDD) is used because PDD is capable of detecting almost all kinds

of gases (organic and inorganic gases) and its sensitivity is much higher than that of TCD. Generally, the PDD signal is approximately one thousand times larger than that of TCD for the same compound. In the review paper of Forsyth (2004), He-PDPID (referred to as PDD in this paper) typically achieved minimum detectable quantities (MDQs) in the low picogram range, while the MDQs of TCD were typically not lower than one nanogram.

In this study, a combined GC and MS device was constructed to allow detecting of  $H_2$ ,  $CH_4$ ,  $H_2O$ , CO,  $N_2$ ,  $C_2H_4$ ,  $C_2H_6$ ,  $O_2$ ,  $H_2S$ , Ar,  $CO_2$ ,  $C_3H_8$ , COS and  $SO_2$  trace gases. To validate the performance of this new device, serpentinized peridotite samples, volcanic lava samples, and shale samples were tested. The data on the serpentine peridotite samples was compared with Zhang et al. (2016) in section 5.1. No suitable data of the volcanic lava samples and the shale samples for comparison has been found.

## 2. ANALYTICAL DEVICES

Figure 1 shows a schematic of the transfer line for extraction and chemical analysis of fluid inclusion gases from rock samples. Rock or mineral samples are degassed by crushing or heating under high vacuum and a manometer measures the gas mixture pressure. The gas mixture is then sent to a mass spectrometer and a sample loop separately, and MS and GC are used to measure the chemical composition of the gas mixture individually.

The device is characterized by high vacuum and small volume and allows releasing gases from samples by crushing and heating. The highest temperature depends on the furnace. The vacuum is below  $10^{-4}$  Pa to avoid outside air interference. The volume is  $124\text{ cm}^3$  and this facilitates the collection of more gas in the sample loop, which improves the overall sensitivity of the instrument. The gas chromatograph uses a PDD detector to further improve instrument sensitivity. In the current iteration of the device, the highest furnace temperature is  $1000^\circ\text{C}$ , but the temperature and volume are subject to changes in the future, if needed for further optimization.

The injection of standard gas from the gas inlet can establish both the relationship curve between the pressure and gas volume of the manometer, but also the relationships between the MS peak intensity, GC peak area and the content of a single compound in the gas mixture. Because the pressure measured by the manometer is independent of the type of gas, the relative curve of a given gas pressure and volume is adaptable to other types of gas. By this method, Colin et al. (2013) estimated the quantity of  $CO_2$  in individual MORB vesicles.

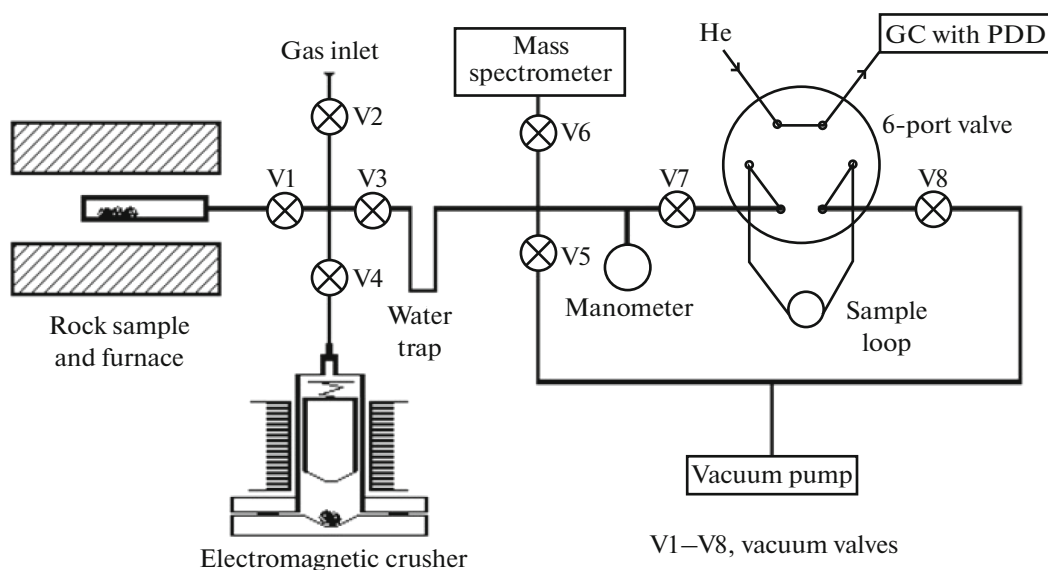


**Fig. 1.** Schematic figure of the device for rock degassing and gas chemical composition analysis by GC and MS. The gas inlet is for standard sample. The electromagnetic crusher works at 50 Hz with a tank inner diameter of 28mm, a piston weight of 125 g and a gasket of oxygen-free copper.

### 3. ANALYTICAL PROCEDURES

#### 3.1. Gas Chromatograph

A GC-9560 (Shanghai Huaai Co., LTD.) gas chromatograph was used and the high-purity He (>99.999%, carrier gas) was further purified with a purifier (HP-2, VICI Co., LTD). The PDD detector (VICI Co., LTD), was set to operate at 250°C. Column 1 was a Porapak Q at 2 m \* 1/16" with the temperature program set as follows: hold for 5 min at 110°C, heat at 10°C/min to 240°C, hold for 12 min at 240°C. Column 2 was a 5A molecular sieve at 0.5 m \* 1/8" and was set to hold a constant temperature of 60°C.

#### 3.2. Mass Spectrometer

In this device, two kinds of mass spectrometers were tested for the chemical analysis of fluid inclusion gases: a quadrupole mass spectrometer, (QMG220, Pfeiffer Vacuum Co. Ltd.) and an ion trap mass spectrometer (835 VQM™, Brooks Co. Ltd.).

#### 3.3. Experimental Procedures

For crushing procedures, an approximately 5 g (0.5–1.5 cm in diameter) rock sample was placed inside a high vacuum electromagnetic crusher and crushed for 0.5–6 minutes, followed by pressure and gas composition analysis of the released gas mixture. The weight, size of the rock sample, and crushing time varied among the samples, depending on several factors including the rock type, total gas content, and/or differing test objectives, among others.

For heating procedures, an approximately 0.2 g (0.18–0.5 mm in diameter) rock sample was step heated in a high vacuum quartz tube, with each step heating for about 50 min, followed by pressure and gas composition analysis of the released gas. Again, the weight, size of the rock sample, step temperature, and heating time varied to some degree, depending on the same factors affecting crushing procedures (i.e. rock type, total gas content, and/or differing test objectives, among others).

For each gas sample, the pressure was measured by a manometer, and the chemical composition was determined simultaneously by GC and MS.

### 4. BLANK AND SAMPLE TESTS

A step heating blank test was carried out once. The procedure was identical to the step heating tests for the experimental samples except that it was carried out with no sample. Detailed step heating experiments and data processing are described in Section 5.2. The step heating blank test data do not need to be processed separately, and a simple spectral subtraction method may be used. Most GC and MS have their own spectra subtraction means.

#### 4.1. Crushing Blank Test

The sample tank in the electromagnetic crushing device was baked at 400°C for 14 h to remove water and organic matter absorbed on the surfaces of the tank. An approximately 1 mm, 4.52 g quartz sample that was baked at 900°C for 14 h was used for the crushing test blank sample. This sample was crushed

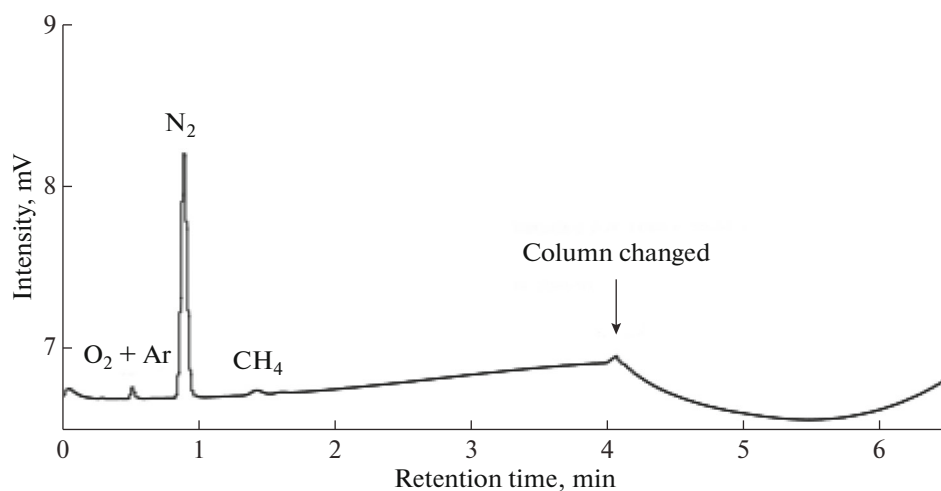


Fig. 2. GC spectra of gases released from blank sample by crushing.

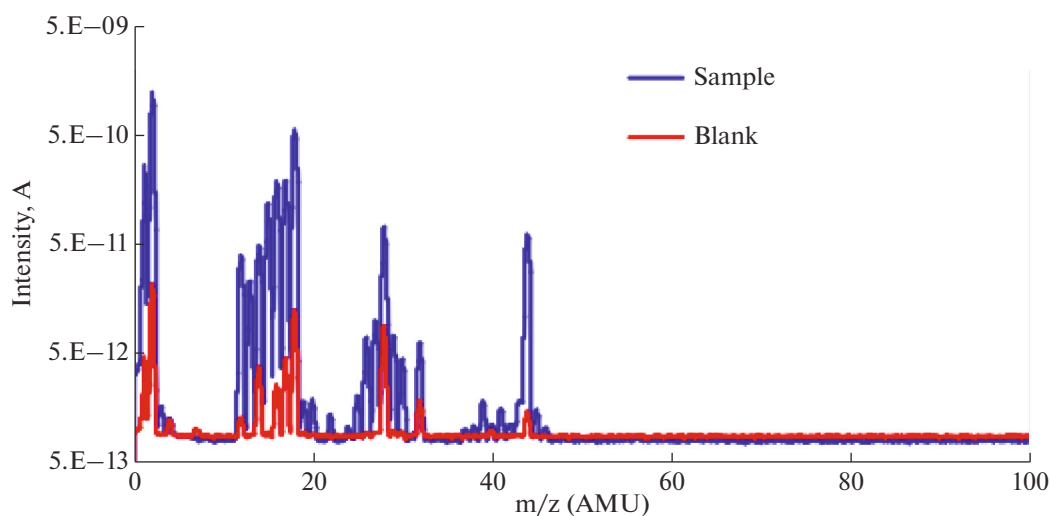


Fig. 3. MS spectra of gases released from a rock sample and a blank sample by crushing. The unit resolution at 10% peak height is 0.5 u.

for 2 min, with a maximum temperature of the outer wall of the sample tank of 37°C. The gas released pressure was 0.5 Pa, corresponding to 0.62 mm<sup>3</sup> STP (where STP is taken as approximately 20°C and 1 atm). The main component measured by GC is nitrogen (Fig. 2). One can see from Fig. 2, that the ratio of N<sub>2</sub> to O<sub>2</sub>+Ar is different from that found in air, demonstrating that the gas measured in the tank was not solely from air in the tank, and that there may have been a small amount of residual N<sub>2</sub> released from the blank sample during crushing. By comparing the ratio of O<sub>2</sub>+Ar in the blank sample to the known ratio of O<sub>2</sub>+Ar in air, the air content was estimated to be 13%. This suggests that 0.08 mm<sup>3</sup> STP of air may be leaked during the crushing process. Accordingly, a detection limit of 0.1 mm<sup>3</sup> STP is suggested. Temperature was clearly an

important parameter with regard to gas absorption into rock, so the temperature of the outer wall of the sample tank was monitored in all the crushing experiments by a K-type thermocouple.

#### 4.2. Sample Test of Crushing

The test sample was from Xushen 1-2, a reservoir rock from the Xujiaweizi Fault-depression located in the northern Songliao Basin, northeastern China (Wang, W. G. et al. 2016). About 5.9 g of sample was crushed for 2 min and the gas was collected. During crushing, the maximum temperature of the outer wall of the sample tank was 51°C, and 129 mm<sup>3</sup> STP of gas was released. Figure 3 shows the MS spectra of the gases from sample and from the blank. The GC spec-

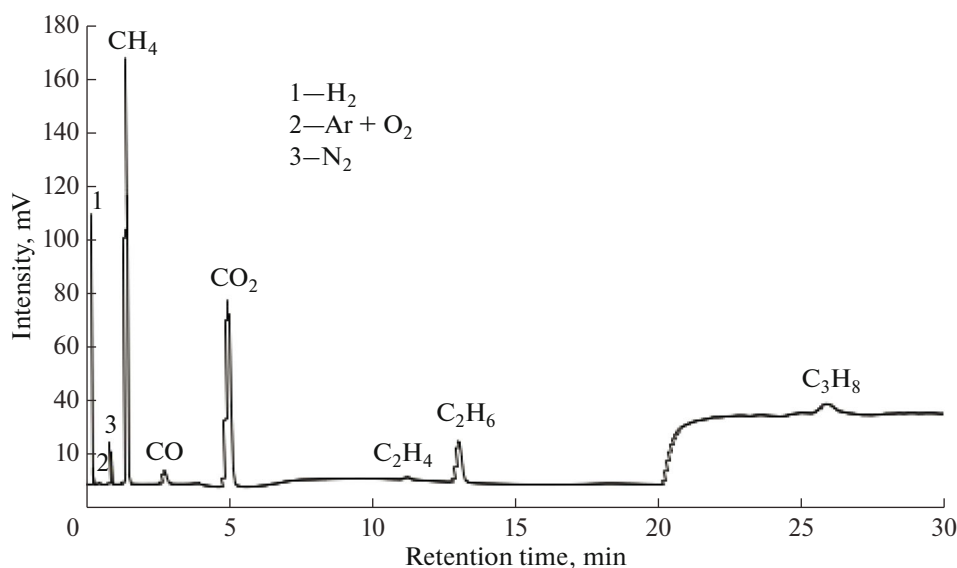


Fig. 4. GC spectrum of gas released from the same rock sample of Fig. 3.

trum of the gas released from the same sample is shown in Fig. 4.

As shown in Fig. 3, or by comparing Figs. 2 and 4, the amount of gas released by the actual rock sample was much more than the amount of gas released by the blank sample. The main components of the gas released from this reservoir rock sample by crushing were  $H_2$ ,  $CH_4$ ,  $N_2$ ,  $C_2H_6$  and  $CO_2$ . Ar was low, which suggests that the air leakage in the crushing process was negligible.

#### 4.3. GC and MS Reproducibility and Linearity

Generally, reference samples are used to test instrument performance. It is unnecessary and sometimes impossible to test all components found in GC and MS. We used air as a reference gas for the GC and MS reproducibility and linearity tests because air is easily obtained and the composition of air is relatively stable.

Li et al. (2016) used air as the reference gas, and the linearity of the QMG220 mass spectrometer was tested. Within the air volume range of 5–30 mm<sup>3</sup> STP, the linear correlation factor of peak intensities of  $N_2$ ,  $O_2$ , Ar and  $CO_2$  were 0.9998, 0.9998, 0.9998 and 0.9783,

respectively, demonstrating that the QMG220 mass spectrometer was suitable for detection of these gases.

In this work, using air as the reference gas, the reproducibility and linearity of the ion trap mass spectrometry were tested. By repeatedly injecting 200 mm<sup>3</sup> STP of air into the device and subsequently measuring  $N_2$ ,  $O_2$  and Ar, the relative standard deviations of relative intensity were 0.34, 0.66 and 1.32%, respectively (Table 1). Within the volume range of 18–327 mm<sup>3</sup> STP, the relative standard deviations of relative intensity were 0.8, 2.4 and 8.4%, respectively (Table 2), demonstrating that the ion trap mass spectrometer was also suitable for detection of these gases.

The reproducibility and linearity of the gas chromatograph were also tested by using air as the reference gas. By repeated measurements of about 100 mm<sup>3</sup> STP air, the relative standard deviations of  $N_2$  and  $O_2+Ar$  relative intensities were 0.63 and 2.2%, respectively (Table 3). Within the volume range of 20–200 mm<sup>3</sup> STP, the linear correlation factors of  $N_2$  and  $O_2+Ar$  peak areas of the gas chromatograph were  $R^2 = 0.98$  and  $R^2 = 0.99$ , respectively (Fig. 5).

Table 1. Reproducibility of the ion trap mass spectrometer

<i>m/z</i>	Test no.								Average	RSD%
	1	2	3	4	5	6	7	8		
28	0.6915	0.6872	0.6920	0.6890	0.6863	0.6885	0.6851	0.6834	0.6879	0.34
32	0.2872	0.2899	0.2870	0.2886	0.2913	0.2891	0.2933	0.2927	0.2899	0.66
40	0.0160	0.0155	0.0156	0.0156	0.0156	0.0155	0.0149	0.0160	0.0156	1.32

**Table 2.** Linearity of the ion trap mass spectrometer

$m/z$	Amount of air, mm <sup>3</sup>								Average	RSD%
	18	49	98	140	172	232	260	327		
28	0.6611	0.6671	0.6621	0.6589	0.6580	0.6521	0.6517	0.6466	0.66	0.8
32	0.3114	0.3158	0.3223	0.3257	0.3296	0.3327	0.3349	0.3413	0.33	2.4
40	0.0154	0.0146	0.0154	0.0154	0.0125	0.0152	0.0134	0.0121	0.01	8.4

**Table 3.** Reproducibility of the gas chromatograph (with 0.1 cm<sup>3</sup> STP of air)

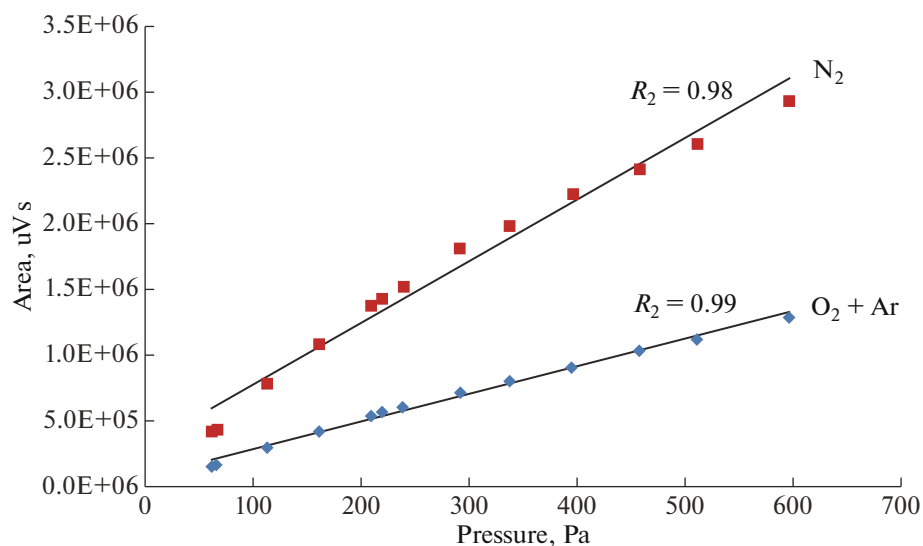
$m/z$	Test no.						Average	RSD%
	1	2	3	4	5	6		
O <sub>2</sub> + Ar	22.52	22.22	21.37	21.45	21.78	21.44	21.8	2.2
N <sub>2</sub>	77.38	77.69	78.57	78.48	78.16	78.49	78.13	0.63
CO <sub>2</sub>	0.092	0.08	0.048	0.058	0.051	0.062	0.065	26.4

## 5. APPLICATION

### 5.1. Step-heating and Degassing of Serpentinized Peridotite Samples

The serpentinized peridotite samples were collected from inner Mongolia (Wang, X. B. et al. 2016). A 0.01 g serpentinized peridotite sample (MC21) was put into a quartz tube and was step-heated to 200, 400, 600, 800 and 1000°C. Each step was held for 50 min. At 200°C, 0.46 mm<sup>3</sup> STP of gas was released and the main components detected by GC and MS were H<sub>2</sub>O, CO<sub>2</sub>, H<sub>2</sub>, N<sub>2</sub>, CH<sub>4</sub> and O<sub>2</sub>. At 400°C, 2.86 mm<sup>3</sup> STP of gas was released and the main components detected by GC and MS were H<sub>2</sub>, H<sub>2</sub>O, CO<sub>2</sub>, N<sub>2</sub>, O<sub>2</sub> and CH<sub>4</sub>. At 600 and 800°C, the main component detected by MS was H<sub>2</sub>O. At 1000°C, some SO<sub>2</sub> was released. Another serpentinized peridotite sample (MC24) was analyzed

according the same procedure as MC21. Figure 6 shows the change of the relative content of the main gas components in the two samples with temperature. The two samples have too much H<sub>2</sub>O released at 600 and 800°C, and the content of O<sub>2</sub> is very low over 400°C, so H<sub>2</sub>O and O<sub>2</sub> are not included in Fig. 6. Figure 7 is a comparison with the Zhang et al. (2016). They used a large magnetic mass spectrometer (Model MAT271) and did not measure water content, and each sample weighed about 0.5 g. From Fig. 7, one can see that the gas release pattern in this work is similar to that of Zhang et al. (2016). In Zhang et al. (2016), It is difficult to determined amounts of CO and CH<sub>4</sub> because the contents of CO and CH<sub>4</sub> is very low, MS cannot effectively separate CO<sup>+</sup> and N<sub>2</sub><sup>+</sup> ions, and CH<sub>4</sub><sup>+</sup> is affected by fragments ions, while in this work it

**Fig. 5.** Relationship of GC area and gas pressure (approximately 20–200 mm<sup>3</sup> of air).

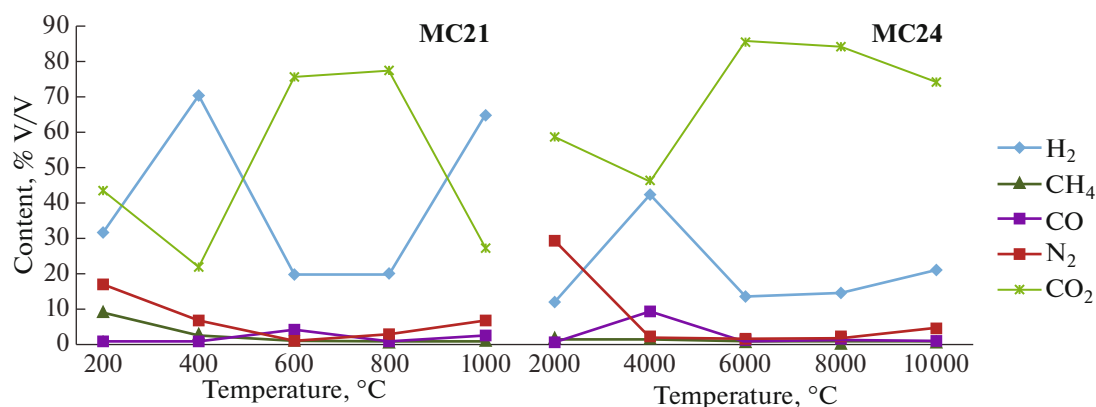


Fig. 6. Gases released from two serpentinized peridotite samples by stepwise heating.

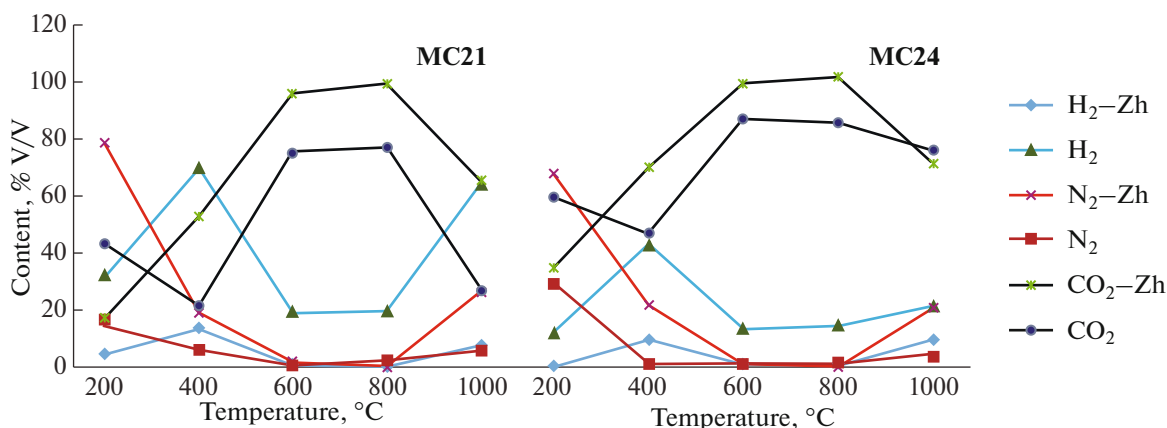


Fig. 7. Comparison of  $H_2$ ,  $N_2$  and  $CO_2$  released from serpentinized peridotite samples by stepwise heating. The data with “-Zh” identification at the end of each component comes from Zhang et al. (2016).

is not a problem. In addition, the amount of rock samples in this work is far less than theirs.

In previous unpublished experiments, a large amount of  $H_2$  was produced in the preparation of rare gas isotope samples by step-heating serpentinized peridotite, which interfered with the test of helium isotope compositions. In the above experiments, the serpentinized peridotite released a large amount of  $H_2O$  under high temperature. It is likely that the  $H_2O$  released under high temperature may have reacted with the crucible during the preparation of the rare gas isotope samples to produce  $H_2$ . If this is the case, the preparation system of rare gas isotopic samples could be improved to meet the requirements for serpentinized peridotite or similar samples by following the sample preparation discussed herein.

### 5.2. Step Heating and Degassing of Volcanic Lava Samples

Step heating experiments were carried out on two samples from Wudalianchi: a Yaoquanshan volcano lava sample and a Huoshaoshan volcano lava sample

(Fig. 8). A quartz tube was pre-heated at  $1000^\circ\text{C}$  in high vacuum before use. Approximately 0.2 g (0.18–0.5 mm in diameter) of each sample was loaded into the quartz tube and held under vacuum for more than 4 h. The sample was then heated from room temperature to  $200^\circ\text{C}$ . After holding the temperature at  $200^\circ\text{C}$  for about 50 min, the gas pressure was measured and the released gas was collected and analyzed by GC for chemical composition. The residual gas was pumped out after entering the GC, and the sample was then heated to  $400^\circ\text{C}$ . After each heating step, the process of holding for 50 minutes followed by pressure determination and sample collection for composition analysis was repeated until a final temperature of  $1000^\circ\text{C}$  was reached. The same steps were followed with the blank sample. The blank-corrected concentration in the sample is expressed in Eq. (1).

$$C(x, T) = Cm(x, T) - B(x, T), \quad (1)$$

where  $Cm(x, T)$  is the measured concentration of a given chemical component  $x$  in the rock sample at a given temperature  $T$ ,  $B(x, T)$  is the concentration of this chemical component in the blank at the same temperature, and  $C(x, T)$  is the blank-corrected con-

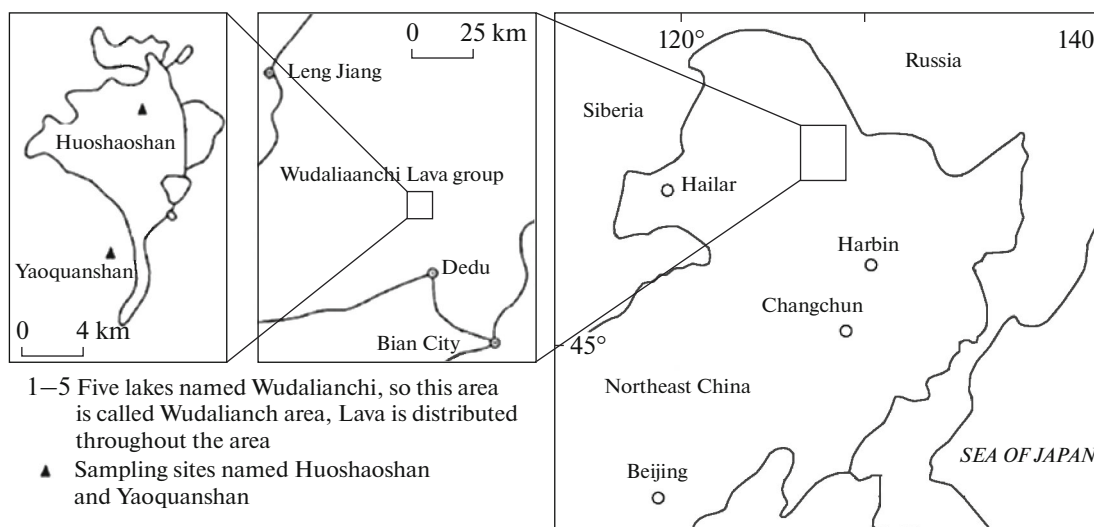


**Fig. 8.** Sample collection sites. Filled triangles are the locations of samples used in this study. Sample H01 from Huoshaoshan, sample Y01 from Yaoquanshan (modified after Liu and Lang, 2011).

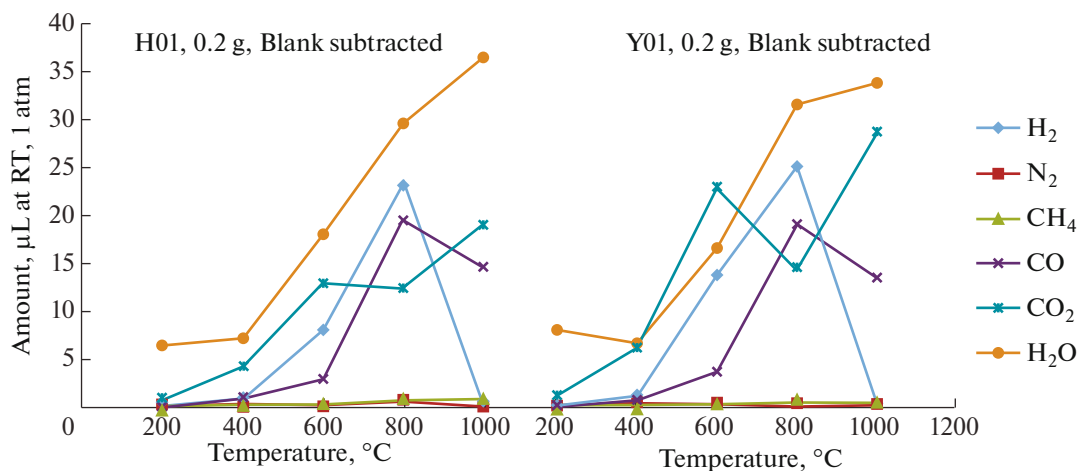


**Fig. 9.** Chemical compositions of gases released by step-heating the Huoshaoshan volcano lava sample (H01) and Yaoquanshan volcano lava sample (Y01). The amounts are in  $\mu\text{L}$  ( $= \text{mm}^3$ ) at room temperature (RT, 20–25°C) and 1 atm.

centration.  $C(x, T)$ ,  $Cm(x, T)$  and  $B(x, T)$  are all measured in microliters ( $\mu\text{L} = \text{mm}^3$ ). Figure 9 shows the results, where the Y-axis (Amount) represents  $C(x, T)$  in Equation (1).

The dominant components of gases released by step heating from the Wudalianchi volcano lava sample were  $\text{H}_2\text{O}$ ,  $\text{CO}_2$ ,  $\text{H}_2$  and  $\text{CO}$ , followed by trace amounts of  $\text{CH}_4$  and  $\text{N}_2$  (Fig. 9). As the temperature increased, the concentration and partial pressure of both  $\text{H}_2\text{O}$  and  $\text{CO}_2$  increased. The concentration of  $\text{H}_2\text{O}$  never plateaued at a maximum through all the heating steps up to 1000°C. This suggests that there was significant  $\text{H}_2\text{O}$  (or possibly another form of H and O in this stoichiometric ratio) in the samples. Esposito et al. (2016) reheated olivine-hosted mafic

melt inclusions from Mt. Somma-Vesuvius, Italy and found liquid  $\text{H}_2\text{O}$  in vapor bubbles in reheated melt inclusions. It is possible that the same phenomena occurred in the Wudalianchi volcano lava samples. The lower  $\text{N}_2$  observed also indicated that there was less nitrogen in the samples and also little air pollution from the gases extracting system.  $\text{H}_2$  and  $\text{CO}$  each have a peak at 800°C and it is possible that a phase change occurred in the samples near 800°C, causing an explosion of fluid inclusions. The relationship between the concentration of oxygen-containing compounds and hydrogen-containing compounds reflects the redox state of volcanic rocks (Huizenga, 2001; Zhang and Duan, 2009), and the depth of volcanic magma and its temperature and pressure conditions can be inferred



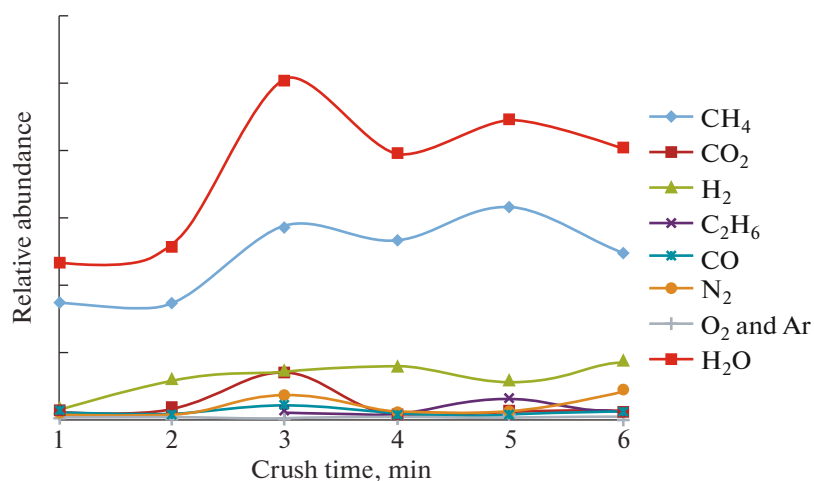


**Fig. 10.** Amount of gases in each component varies with the different crushing time under the same conditions (different aliquots of the same shale, weight and temperature).

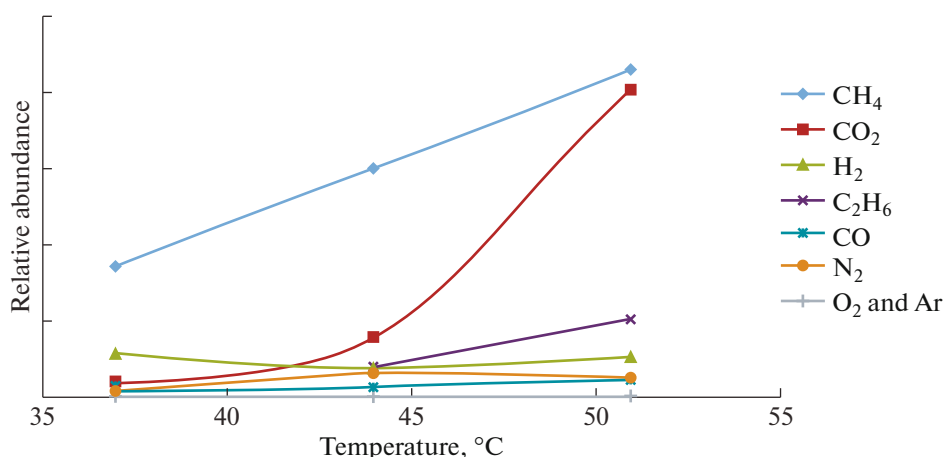


**Fig. 11.** Under the same conditions (sample, weight and crushing time), the gas composition varied with temperature of the sample tank.

from the chemical composition of the gas (Kuritani et al., 2011; Armstrong et al., 2015). Therefore, combining these pieces of information provides the means for understanding the genesis and evolution of the volcano.

### 5.3. GC Tests of Gases Released by Crushing Shale Samples

The shale samples were collected from the Sichuan basin in China. The relationship between the crushing time and the amount of gas released was investigated (Fig. 10). The amount of gas, CH<sub>4</sub>, CO<sub>2</sub>, H<sub>2</sub> and N<sub>2</sub> all increased with increasing crushing time up to a crushing time of 3 minutes, when gas concentrations reached their maxima. As the crushing continued, the GC peak area of each component plateaued. For different samples, the crush time required to reach maximum gas release may be different. As shown in Fig. 11, under the

same conditions (sample, weight and crushing time), the gas composition varied with temperature. The results showed that the CH<sub>4</sub> and CO<sub>2</sub> concentrations increased quickly with small changes in temperature. This may be caused by the adsorption and desorption of the rock powder.

As shown in Fig. 12, the total amount of CH<sub>4</sub>, CO<sub>2</sub> and CO released during step crushing was greater than that of continuous crushing, while the total amount of H<sub>2</sub> and N<sub>2</sub> released during step crushing was less than that of continuous crushing. The most likely explanation for CO<sub>2</sub> is that it is effectively adsorbed onto the newly formed surface. The sorption time at step crushing was 6 times less (at every step) than at continuous single step crushing. Further, it is known that polar molecules are better adsorbed than non-polar ones. The gas pressure at each stage of step crushing was lower than that of continuous crushing, which sug-

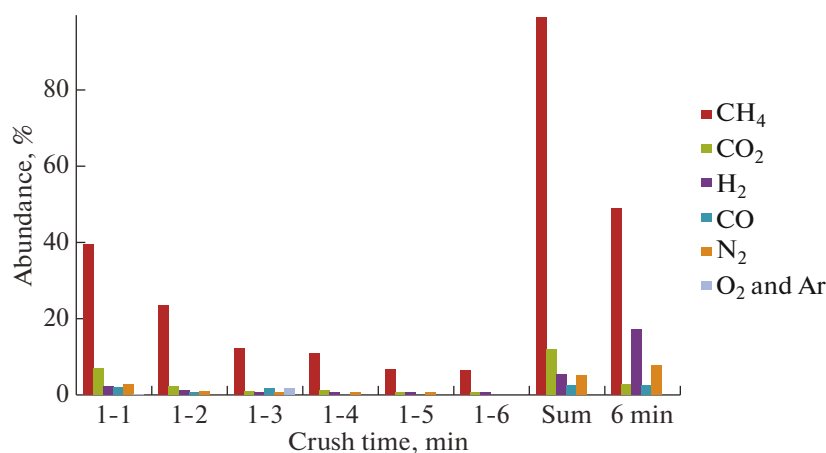


**Fig. 12.** Comparison of gas quantity released by step crushing and continuous crushing. Step crushing was performed in six steps, with each step lasting for one minute, followed by GC testing and pumping out the residual gases. Continuous crushing lasted for six minutes, with the temperature kept between 25–45°C during this time. The sums of the six steps of each component are also shown.

gests that reduced pressures may encourage the release of polar molecules (e.g. CH<sub>4</sub>, CO<sub>2</sub> and CO) and discourage the release of non-polar molecules (e.g. H<sub>2</sub> and N<sub>2</sub>). Zhang, T. W. et al. (2014) showed that both thermal maturity and gas desorption contributed to changes in the CH<sub>4</sub>/CO<sub>2</sub> ratio of gases released during rock crushing.

Table 4 shows the GC results of the chemical composition of gases released from seven shale samples. Low O<sub>2</sub>+Ar content indicated that the vacuum seal of the system was very good. Li et al. (2017) analyzed the chemical composition of gases released from some shale samples with GC: There were different kinds of gas assemblages in different shale samples and varied in composition from exhibiting mainly CH<sub>4</sub>, to mainly CO<sub>2</sub>, to showing high concentrations of H<sub>2</sub> or N<sub>2</sub>. A similar conclusion can be obtained from Table 4.

## 6. CONCLUSIONS

A new device was built that was capable of measuring trace gases extracted from rock samples by GC and

MS together, with the use of a highly sensitive PDD used for detection by GC. Volcanic lava samples, serpentinized peridotite samples and shale samples were tested to validate the utility of the device, and the chemical contents of H<sub>2</sub>, CH<sub>4</sub>, H<sub>2</sub>O, CO, N<sub>2</sub>, C<sub>2</sub>H<sub>4</sub>, C<sub>2</sub>H<sub>6</sub>, O<sub>2</sub>, H<sub>2</sub>S, Ar, CO<sub>2</sub>, C<sub>3</sub>H<sub>8</sub>, COS and SO<sub>2</sub> released from rock samples could all be measured at one time with a detection limit of 0.1 mm<sup>3</sup> STP. It was indicated from the above that the chemical contents of H<sub>2</sub>, CH<sub>4</sub>, CO, N<sub>2</sub>, C<sub>2</sub>H<sub>4</sub>, C<sub>2</sub>H<sub>6</sub>, O<sub>2</sub>+Ar, CO<sub>2</sub>, C<sub>3</sub>H<sub>8</sub> can be determined by GC, while O<sub>2</sub>, H<sub>2</sub>S, Ar, COS and SO<sub>2</sub> may be determined by MS. Some gases were not detected in the experiment, such as H<sub>2</sub>S, COS and SO<sub>2</sub>, but they should be able to be detected if in high enough abundances. Complications arose, however, with the electromagnetic crusher, which could not be heated. Additionally, gas adsorption was observed on the surface of rock samples after discharge, causing changes in gas volume and composition, which may not truly reflect the result of degassing. The highest temperature of the step heating furnace was 1000°C, and H<sub>2</sub>O release from volcanic samples was incomplete. While

**Table 4.** Chemical composition of gases released from shale by crushing

Sample no.	Abundance of gas, %								
	H <sub>2</sub>	O <sub>2</sub> +Ar	N <sub>2</sub>	CH <sub>4</sub>	CO	CO <sub>2</sub>	C <sub>2</sub> H <sub>4</sub>	C <sub>2</sub> H <sub>6</sub>	C <sub>3</sub> H <sub>8</sub>
1	20.48	0.20	6.37	9.25	0.20	63.46	0.00	0.04	0.00
2	34.82	0.39	18.22	3.12	3.00	40.39	0.00	0.05	0.00
3	15.02	0.37	17.19	60.77	0.62	6.03	0.00	0.00	0.00
4	61.28	0.22	13.14	8.35	2.31	14.52	0.00	0.17	0.00
5	2.51	0.00	0.13	1.66	1.08	94.45	0.01	0.13	0.02
6	54.98	1.14	5.28	38.37	0.03	0.04	0.00	0.11	0.05
7	4.09	0.04	1.48	28.97	0.00	65.31	0.00	0.11	0.00

this work has demonstrated advancement toward more complete analyses of gases trapped in rock and mineral samples, future improvements are clearly needed.

#### ACKNOWLEDGMENTS

We would like to thank O. F. Mironova, D.t.n. V. S. Sevastyanov and an anonymous reviewer for their reviews and constructive suggestions. This study was supported financially by NSF of China (no. 41473062) and the Key Laboratory Project of Gansu Province (Grant no. 1309RTSA041).

#### REFERENCES

- L. S. Armstrong, M. M. Hirschmann, B. D. Stanley, E. G. Falksen, S. D. Jacobsen, "Speciation and solubility of reduced C–O–H–N volatiles in mafic melt: Implications for volcanism, atmospheric evolution, and deep volatile cycles in the terrestrial planets," *Geochim. Cosmochim. Acta* **171**, 283–302 (2015).
- N. J. F. Blamey, "Composition and evolution of crustal, geothermal and hydrothermal fluids interpreted using quantitative fluid inclusion gas analysis," *J. Geochem. Explor.* **116–117**, 17–27 (2012).
- A. I. Buikin, A. I. Kamaleeva, and N. A. Migdisova, "Prospects of the method of stepwise crushing as a source of information on the fluid phase of rocks and minerals," *Petrology* **24** (3), 303–313 (2016).
- Clay, P. L. H. Busemann, and S. C. Sherlock, "<sup>40</sup>Ar/<sup>39</sup>Ar ages and residual volatile contents in degassed subaerial and subglacial glassy volcanic rocks from Iceland," *Chem. Geol.* **403**, 99–110 (2015).
- A. Colin, P. Burnard, and B. Marty, "Mechanisms of magma degassing at mid-oceanic ridges and the local volatile composition (<sup>4</sup>He–<sup>40</sup>Ar\*–CO<sub>2</sub>) of the mantle by laser ablation analysis of individual MORB vesicles," *Earth Planet. Sci. Lett.* **361**, 183–194 (2013).
- Doucet, L. S. A. H. Peslier, D. A. Ionov, A. D. Brandon, A. V. Golovin, A. G. Goncharov, and I. V. Ashchepkov, "High water contents in the Siberian cratonic mantle linked to metasomatism: an FTIR study of Udachnaya peridotite xenoliths," *Geochim. Cosmochim. Acta* **137**, 159–187 (2014).
- Y. V. Dublyansky, "Design of two crushing devices for release of the fluid inclusion volatiles," *Central Eur. J. Geosci.* **4** (2), 219–224 (2012).
- Esposito, R. J. Hunter, J. D. Schiffbauer, and J. R. Bodnar, "An assessment of the reliability of melt inclusions as recorders of the pre-eruptive volatile content of magmas," *Am. Mineral.* **99** (5–6), 976–998 (2014).
- R. Esposito, H. M. Lamadrid, D. Redi, et al., "Detection of liquid H<sub>2</sub>O in vapor bubbles in reheated melt inclusions: Implications for magmatic fluid composition and volatile budgets of magmas?," *Am. Mineral.* **101**, 1691–1695 (2016).
- T. P. Fischer and B. Marty, "Volatile abundances in the sub-arc mantle: insights from volcanic and hydrothermal gas discharges," *J. Volcanol. Geotherm. Res.* **140** (1/3), 205–216 (2005).
- D. S. Forsyth, "Pulsed discharge detector: theory and applications," *J. Chromatogr. A* **1050**, 63–68 (2004).
- M. L. Frezzotti, F. Tecce, and A. Casagli, "Raman spectroscopy for fluid inclusion analysis," *J. Geochem. Explor.* **112**, 1–20 (2012).
- S. A. Halldórsson, D. R. Hilton, P. H. Barry E. Füre, and K. Grönvold, "Recycling of crustal material by the Iceland mantle plume: new evidence from nitrogen elemental and isotope systematics of subglacial basalts," *Geochim. Cosmochim. Acta* **176**, 206–226 (2016).
- J. M. Huizenga, "Thermodynamic modelling of C–O–H fluids," *Lithos* **55**, 101–114 (2001).
- F. Klein, W. Bach, and T. M. McCollom, "Compositional controls on hydrogen generation during serpentinization of ultramafic rocks," *Lithos* **178**, 55–69 (2013).
- T. Kuritani, E. Ohtani, J. I. Kimura, "Intensive hydration of the mantle transition zone beneath China caused by ancient slab stagnation," *Nature Geosci.* **4**, 713–716 (2011).
- L. W. Li, L. J. Guo, Y. Q. Xia, and J. C. Tuo, "Development of an automatic gas sampler for trace analysis by mass spectrometer. Modern Scientific Instruments," No. 6, 85–89 (2016) (in Chinese with English abstract).
- L. W. Li, Y. Liu, X. B. Wang, M. J. Zhang, C. H. Cao, L. T. Xing, Z. P. Li, "Development of a combined device with high vacuum and pulsed discharge gas chromatography and its application in chemical analysis of gases from rock samples," *Rock Mineral Anal.* **36** (3), 222–230 (2017) (In Chinese with English abstract).
- G. Liu, X. B. Wang, and L. W. Li, "Chemical composition of gas from mantle xenoliths in alkali-basalt from Damaping, Hebei," *Chin. Sci. Bull.* **42** (6), 470–472 (1997).
- X. Liu and J. J. Lang, "Discovery of volcanic debris-avalanche deposits in Laohei and Huoshao volcanoes, Wudalianchi world geopark, and ascertaining the volcanoes' history and eruptive model again," *Geol. Rev.* **57** (5), 650–658 (2011) (in Chinese with English abstract).
- B. Marty, and F. Humbert, "Nitrogen and argon isotopes in oceanic basalts," *Earth Planet. Sci. Lett.* **152**, 101–112 (1997).
- G. Menard, S. Moune, I. Vlastélic, F. Aguilera, S. Valade, M. Bontemps, and R. González, "Gas and aerosol emissions from Lascar volcano (Northern Chile): Insights into the origin of gases and their links with the volcanic activity," *J. Volcanol. Geotherm. Res.* **287**, 51–67 (2014).
- J. K. Mi, K. He, S. Z. Tao, C. Yang, and M. M. Sun, "Geochemical comparison between the gas in bulk fluid inclusions and reservoir gas produced in Paleozoic formation, Ordos Basin, China," *J. Geochem. Explor.* **171**, 133–140 (2016).
- O. F. Mironova, "Volatile components of natural fluids evidence from inclusions in minerals methods and results," *Geochem. Int.* **48** (1), 83–90 (2010).
- I. Mulder, S. G. Huber, T. Krause, C. Zetzsch, K. Kotte, S. Dultz, and H. F. Schöler, "A new purge and trap headspace technique to analyze low volatile compounds from fluid inclusions of rocks and minerals," *Chem. Geol.* **358**, 148–155 (2013).
- D. G. Pearson, F. E. Brenker, F. Nestola, J. McNeill, L. Nasdala, M. T. Hutchison, S. Matveev, K. Mather, G. Silversmit, S. Schmitz, B. Vekemans, and L. Vincze, "Hydrous mantle transition zone indicated by ring-

- woodite included within diamond,” *Nature* **507**, 221–224 (2014).
- J. Potter and F. J. Longstaffe, “A gas–chromatograph, continuous flow–isotope ratio mass spectrometry method for  $\delta^{13}\text{C}$  and  $\delta\text{D}$  measurement of complex fluid inclusion volatiles: Examples from the Khibina alkaline igneous complex, northwest Russia and the south Wales coalfields,” *Chem. Geol.* **244**, 186–201 (2007).
- M. Queißer, M. R. Burton, F. Arzilli, A. Chiarugi, G. I. Marliyani, F. Anggara, and A. Harijoko, “ $\text{CO}_2$  flux from Javanese mud volcanism,” *J. Geophys. Res.: Solid Earth* **122**, 4191–4207 (2017).
- S. Salvi, and A. E. Williams–Jones, “Bulk analysis of volatiles in fluid inclusions,” In *Fluid Inclusions: Analysis and Interpretation*, 1st Ed. (Publisher: Mineralogical Association of Canada, 2003), pp. 10–1–10–30.
- A. G. Sokol, Y. N. Palyanov, A. A. Tomilenko, T. A. Bul’bak, and G. A. Palyanova, “Carbon and nitrogen speciation in nitrogen–rich C–O–H–N fluids at 5.5–7.8GPa,” *Earth Planet. Sci. Lett.* **460**, 234–243 (2017).
- Q. Y. Tang, M. J. Zhang, C. S. Li, M. Yu, and L. W. Li, “The chemical compositions and abundances of volatiles in the Siberian large igneous province: constraints on magmatic  $\text{CO}_2$  and  $\text{SO}_2$  emissions into the atmosphere,” *Chem. Geol.* **339**, 84–91 (2013).
- T. Toki, D. Iwata, U. Tsunogai, D. D. Komatsu, Y. Sano, N. Takahata, H. Hamasaki, and J. Ishibashi, “Formation of gas discharging from Taketomi submarine hot spring off Ishigaki Island in the southern Ryukyu Islands, Japan,” *J. Volcanol. Geotherm. Res.* **330**, 24–35 (2017).
- W. G. Wang, M. Wang, S. F. Lu, S. M. Chen, M. Zheng, and X. Z. Wu, “Basin modelling of gas migration and accumulation in volcanic reservoirs in the Xujiaweizi Fault–depression, Songliao Basin,” *Arab. J. Geosci.* **9** (166), 1–24 (2016).
- X. B. Wang, Z. Y. Ouyang, S. G. Zhuo, et al., “Serpentinization, abiogenic organic compounds, and deep life,” *Science China (Earth Sci.)* **57** (05), 878–887 (2014).
- X. B. Wang, S. G. Zhou, and M. F. Zhang, Oxidation–reduction characteristics of the serpentinized peridotite. *Bulletin of Mineralogy, “Petrol. Geochem.”* **35** (2), 231–238 (2016) (in Chinese with English abstract).
- M. J. Zhang, P. Q. Hu, Y. L. Niu, and S. G. Su, “Chemical and stable isotopic constraints on the nature and origin of volatiles in the sub–continental lithospheric mantle beneath eastern China,” *Lithos* **96**, 55–66 (2007).
- C. Zhang and Z. H. Duan, “A model for C–O–H fluid in the Earth’s mantle,” *Geochim. Cosmochim. Acta* **73**, 2089–2102 (2009).
- C. Zhang and Z. H. Duan, “GFluid: An Excel spread sheet for investigating C–O–H fluid composition under high temperatures and pressures,” *Comp. Geosci.* **36**, 569–572 (2010).
- M. F. Zhang, S. G. Zhuo, J. C. Tuo, C. J. Wu, L. N. Sun, Y. Liu, Z. P. Li, L. W. Li, H. X. Chi, and X. B. Wang, “The gas composition and genesis of the serpentinized peridotite in the Wenduermiao area, inner Mongolia, China,” *Bull. Mineral. Petrol. Geochem.* **35** (2), 255–263 (2016) (in Chinese with English abstract).
- M. L. Zhang, Z. F. Guo, L. H. Zhang, Y. T. Sun, and Z. H. Cheng, “Geochemical constraints on origin of hydrothermal volatiles from southern Tibet and the Himalayas: understanding the degassing systems in the India–Asia continental subduction zone,” *Chem. Geol.* **469**, 19–33 (2017).
- T. W. Zhang, R. S. Yang, K. L. Milliken, S. C. Ruppel, R. J. Pottorf, and X. Sun, “Chemical and isotopic composition of gases released by crush methods from organic rich mudrocks,” *Org. Geochem.* **73**, 16–28 (2014).
- G. D. Zheng, S. Xu, S. Y. Liang, P. L. Shi, and J. Zhao, “Gas emission from the Qingzhu River after the 2008 Wenchuan Earthquake, Southwest China,” *Chem. Geol.* **339**, 187–193 (2013).